

## Mineralogical Indicators of Early Iron Age Clay Processing Techniques in Eastern Cameroon: A Pilot Study with Mössbauer Spectroscopy

Dong Hyeok Moon<sup>1</sup>, Zoila Luz Epossi Ntah<sup>2</sup>, Junghyun Um<sup>3</sup>, Hyo-Im Kim<sup>3,4\*</sup>, and Jin-Young Lee<sup>1</sup>

<sup>1</sup>Geological Survey Division Korea Institute of Geoscience and Mineral Resources (KIGAM), Daejeon 34132, Republic of Korea

<sup>2</sup>Department of Arts and Archaeology, Faculty of Arts, Letters and Social Sciences, University of Yaounde 1, 755 Yaounde, Cameroon

<sup>3</sup>Department of Geology, Gyeongsang National University, Jinju 52828, Republic of Korea

<sup>4</sup>Research Institute of Molecular Alchemy, Gyeongsang National University, Jinju 52828, Republic of Korea

(Received 26 September 2025, Received in final form 9 December 2025, Accepted 10 December 2025)

This study investigates the traditional method of pottery production in Mombal, a historically significant region in eastern Cameroon, known for its continuous ceramic practices from prehistoric times through the 19th century. Multiple techniques such as cross-sectional observation, X-ray fluorescence, elemental mapping, X-ray diffraction, and Mössbauer spectroscopy have been used for this study. The mineralogical indicators reveal new information about clay processing, including the selection of raw clay and whether potters added coloring materials in the paste, as well as the firing systems used. In particular, as an archaeo-thermometers, the residual of kaolinite and the aspects of iron-components indicate the irregularities in firing intensity and redox conditions in each part of the pottery cross-section. This suggests the possibility that past potters deliberately chose firing system such as bon-firing and pit-firing during pottery manufacturing in Mombal. These findings demonstrate the effectiveness of Mössbauer spectroscopy in identifying hidden mineralogical indicators in archaeological ceramics, and provide crucial insights into the ceramic tradition of the Mombal region in eastern Cameroon.

**Keywords :** Mössbauer spectroscopy, clay processing, mombal ceramics, mineral indicators, iron-oxides, firing techniques

### 1. Introduction and Archaeological Background

Mombal is located in the eastern region of Cameroon in the Lom et Djerem Division (Fig. 1). Lom et Djerem Division is a transition zone between the forest in South Cameroon and the Savannah in North Cameroon. This region is part of a huge Precambrian granitic plateau (500-1000 m of altitude) which is in parts overlain by Mesozoic sandstone [1]. Valleys running through the plateau favoured the settlement of people. Archaeological studies have attested the early settlements in the eastern region since the Paleolithic due to presence of lithic cores and flakes [2].

During the construction of the Bertoua-Garoua Boulaï national road from 1999 to 2002 [3], more than 130

archaeological sites were discovered in eastern Cameroon. Archaeological rescue in the region attested the presence of settlements from the Late Stone Age to the colonial period in Cameroon: 6000-400 BP (Before Present: 1950) [3]. The first excavations and studies were carried out in Wele Maroua and Mombal [4-6]. According to the literature, Mombal is the most studied area due to its abundance of ceramic artifacts collected during road construction and the presence of ethnographic ceramics [5-7]. The preliminary archaeological research in Wele Maroua focused on the settlements in the site and the description of the artifacts [4]. The archaeological materials consisted mainly of ceramics with macro-vegetal relicts, splinters of quartz, and paleo-metallurgical relicts such as slags and eroded iron tools. The radiocarbon dating of charcoal from this locality gave evidence for an occupation period from  $3359 \pm 80$  BP to  $1350 \pm 70$  BP [4].

The first archaeological research in Mombal site started by Lako in 2005 with the first goal to increase the knowledge on the settlement sites situated in the vicinity

©The Korean Magnetics Society. All rights reserved.

\*Corresponding author: Tel: +82-55-772-1478

e-mail: [hyoim@gnu.ac.kr](mailto:hyoim@gnu.ac.kr)

of the road from Bertoua to Garoua-Boulai [5]. The second goal of Lako's research was to study the structure of these sites with respect to pottery industries and techniques as well as production tools. She found sixteen new sites in Mombal and its surroundings. However, she excavated only two sites (Kpountoumbale and Béoutobale situated around 7km off Mombal Chiefsdom). Although, this region is characterized by the abundance of ceramics artefacts, lithic and metal relicts have been also found in Mombal. Two types of pottery were found in the sites excavated by Lako [5]. For the first group of pottery two dates are given ( $1543 \pm 22$  BP and  $1612 \pm 23$  BP) which means that the sherds are of a similar chrono-cultural period. The age of the second group is  $2165 \pm 52$  BP; the ceramics are altered, not ornamented. These results showed an old tradition of pottery in Mombal site according to the ethnographic study of pottery in the central and eastern Cameroon [8]. Moreover, this region is recognized as a valuable source of evidence for documenting and analyzing ceramic traditions amidst numerous ethnic groups; Gbayas, Mboum, Mkako, kaka,

Kepere, Fulbe and Mboros [8]. According to the literature, the traditional making of Pottery in Lom et Djerem persisted until the late 20th century AD [8]. The research of Lako on the ancient ceramics from Mombal, was focused on the stylistic- morphology and macroscopic approaches to identify their origin and some technological parameters.

The second research carried out on Mombal ceramics has been done by Epossi Ntah with the aim to contribute the knowledge about their provenance and technological aspects [6]. Following standard protocols for archaeo-scientific analyses, she employed a physicochemical approach to characterize a selected group of pottery from Boutil. The analytical methods applied included X-ray diffraction (XRD), X-ray fluorescence (XRF), optical microscopy, scanning electron microscopy (SEM), and thermal analysis (TGA/TG) on bulk samples of both clay and ceramics. As part of this research, an excavation was carried out at Boutil in 2008—one of the sites discovered by Lako [5], an abandoned old village with the coordinates ( $5^{\circ}42'27''$ N and  $14^{\circ}26'34''$ E)—situated about

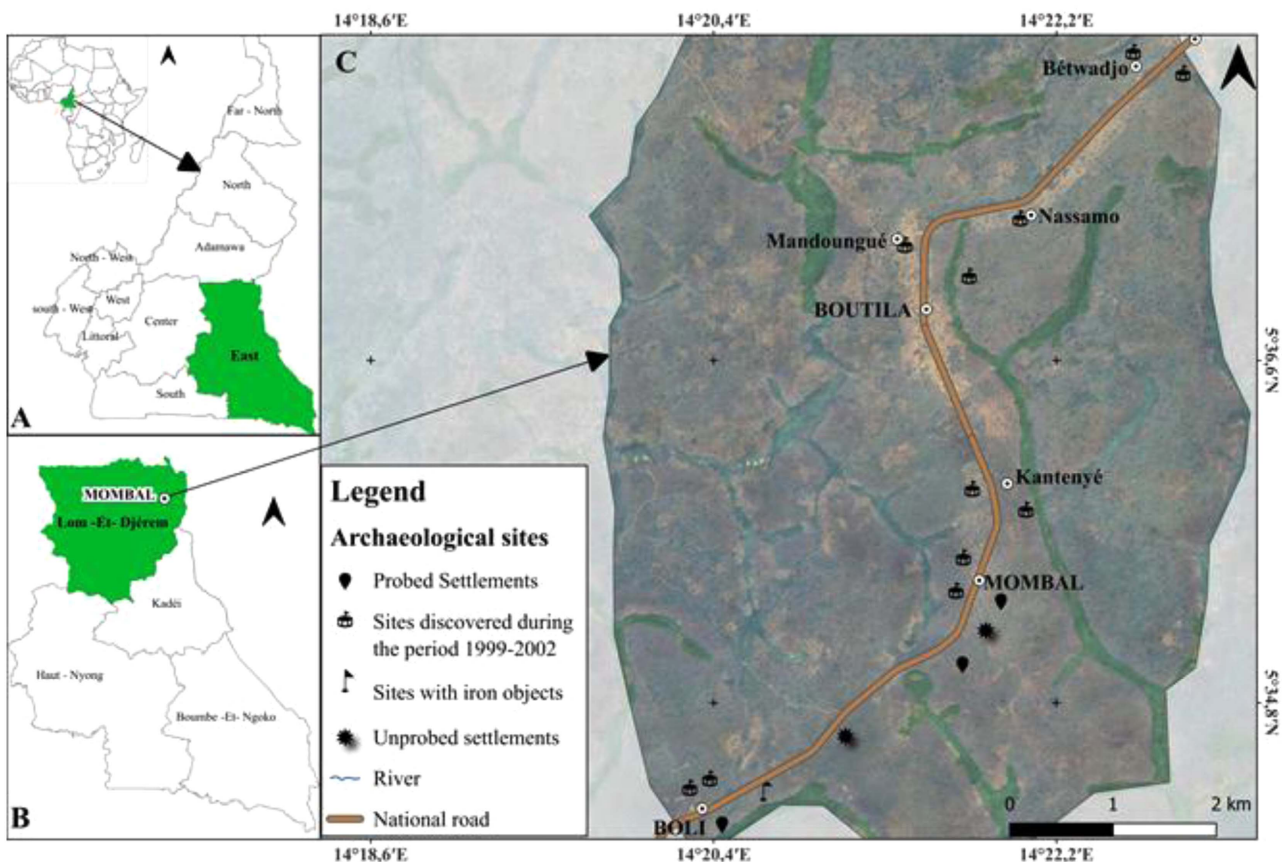


**Fig. 1.** (Color online) General sketch of Africa and location of eastern region in Cameroon: (A) location of Mombal in eastern Cameroon, (B) localization of Mombal, and (C) localization of Boutil and associated sites along the national road Bertoua-Garoua Boulai.

14 km NE off Mombal (Fig. 1). The sampling started on the surface and then layers of 10 cm in thickness were successively removed and the soil searched for ceramics sherds, charcoal, bones, and metallic artefacts (slags) as well as some pottery from the village.

The radiocarbon dating of charcoal collected at the Boutil site yielded an age of  $145 \pm 30$  BP which period is very recent by comparison with the site of Wele Maroua dated from  $3359 \pm 80$  BP to  $1350 \pm 70$  BP [4]. However, the macroscopic characteristics of the pottery sherds recovered from the Boutil site exhibit a strong resemblance to those of the Early Iron Age specimens collected by Lako, which have been radiocarbon-dated to  $1543 \pm 22$  BP and  $1612 \pm 23$  BP [5]. They exhibit consistent characteristics, including color of outer surfaces, surface treatment, impressions as major decoration technique, thickness, and texture of the clay paste [5, 6]. The archaeometric results showed a local production of ceramics from Boutil with a variation of firing temperature ranging below  $600^\circ\text{C}$  and between 600 to  $900^\circ\text{C}$  [6, 7].

Over the past few decades, numerous ethno-archaeological studies have been conducted on the ceramic traditions, ethnohistory, and ethnographical implications of sub-Saharan Africa, including Cameroon; they have focused on reconstructing production techniques and the inspirational interactions between ethnic groups [8-18]. Traditional craft skills are believed to be deeply rooted in the culture and lifestyle of a particular ethnic group [9-22]. Above all, pottery has evolved over time with respect to technology, function, and aesthetics, encompassing diverse information that can provide insights into the chronological background and living conditions of the excavated sites. The form, decoration, color, and mineralogical and chemical composition of the raw materials used in their production serve as informative indicators of the cultural and technological sophistication of the period, highlighting their significance in the study of human history. The study of pottery-making practices represents a highly complex process. Beyond simply analyzing the technical and technological elements involved in the manufacturing, it requires a comprehensive examination of the broader context in which pottery production took place; it must incorporate the broad cultural, social, economic, and political factors that influenced the practices of potters and their groups.

These interpretations, based on *chaînes opératoires*, indicate that the technology of pottery production in this region remained relatively unchanged over time [11, 23]. In addition, the dating presented at the Boutil site coincides with the migration of the Gbaya people, who settled in the area in the 19th century [24, 25]. Moreover,

it also corresponds the date when pottery production ceased in the Mombal region. Therefore, the study of the pottery fragments from this study area holds archaeological significance, as it represents the last Early Iron Age technology-based pottery produced in the Mombal region of eastern Cameroon. It provides the answers to the questions of whether the origins of this Early Iron Age-pottery tradition in the Mombal region can be traced back to earlier times, and how far its roots back.

The present work is a new contribution to the knowledge of archaeological ceramic technology from Mombal region. It is a pilot study focused on technological aspects, especially firing processes of clay paste, by evaluating its mineralogical indicators based on chemical, mineralogical, and magnetic properties. X-ray diffraction, X-ray fluorescence, and Mössbauer spectroscopy have been chosen as analytical methods to conduct the research. Moreover, unlike most previous archaeometric studies that focused primarily on bulk analyses, the present study conducted separately on the two distinct layers observable across the cross-sections of the pottery sherds. The main goal of the work is to develop a hypothesis/model for the oxidation and/or reduction firing history in Mombal. The application of Mössbauer spectroscopic approach on archaeological ceramic sherds is innovative in Mombal and West Africa.

## 2. Experimental

### 2.1. Materials

In this study, three representative sherds, have been selected in the collection of sherds excavated in May 2008 at the site of Boutil [6]. Samples for the Mössbauer spectroscopic analysis as a part of pilot study were selected based on their surface colors, cross-sectional color patterns, and relatively greater thickness (Table 1, Fig. 2). These samples are named S8, S10 and S11. Although the three samples for the current study is not sufficient to ensure the representativeness of the results, the present research will be a reference for the future research using Mössbauer spectroscopy in archaeological samples from Cameroon and central Africa.

**Table 1.** The cross-sectional colors of the representative Mombal pottery sherds.

Sample	Color in fracture surface		Structural type
	Outer part	Body core	
S8	Reddish-brown	Dark brown to grey	Sandwich
S10	Light brown	Dark grey to black	Sandwich
S11	Black	Black	Monochrome

The surface of all the sherds is polished or smoothed. Some of them present charcoal pieces on the outer surface due to the use of the original vessel on the fire. The surface of all sherds is decorated, and the principal trace of decoration techniques is impression and incision with a variety of designs with geometrical patterns. S11 presents a monochrome color cross-section (black) whereas S8 and S10 present a sandwich structure with a brownish surface to dark colored core.

## 2.2. Sample preparation

All samples were prepared as cross-sectional specimens for observation and chemical analysis. As the surfaces (outer and inner) of pottery sherds excavated from archaeological sites are affected by vessel use, surface treatment during manufacture, and subsequent burial history, they do not reliably reflect the firing process. Therefore, our investigations and analyses were carried out on the basis of cross-sectional specimens to ensure the reliability of the results.

In addition, powdered mineral particles were collected to determine the mineral composition of the pottery sherds. We collected particles of each part carefully from the cross-section with a scalpel while observing the light brown to red-brown colored outer rim and grey to black colored core body. The collected mineral particles were not subjected to any separate pretreatment, in order to accurately reflect the entire mineral composition.

## 2.3. Methods

Chemical analyses and elemental distributions were examined using a micro-X-ray fluorescence spectrometer (micro-XRF; M4 TORNADO, Bruker, USA). The operating voltage and current were set at 50 kV and 600  $\mu$ A, respectively. The spot size and step size were fixed at 20  $\mu$ m and 30  $\mu$ m, and the measurement time was set to 10 ms per pixel.

X-ray diffraction analyses (XRD) were performed to determine the bulk mineral composition of the powdered samples. The XRD spectra were recorded using a Cu-K $\alpha$  diffractometer D8 Advanced A25 (Bruker, USA), which scanned in the range of 5°–60° (2 $\theta$ ) at 40 kV and 40 mA with an interval of 0.02° (2 $\theta$ ).

Mössbauer spectroscopy measurements were conducted at the Korea Atomic Energy Research Institute (KAERI). A FAST Mössbauer velocity transducer was used for the measurements, and a proportional counter was employed as the detector. The Mössbauer spectra were recorded at room temperature (RT) using a transmission spectrometer in constant acceleration mode with a  $^{57}\text{Co}/\text{Rh}$  source, calibrated with  $\alpha$ -Fe as a standard and fitted with

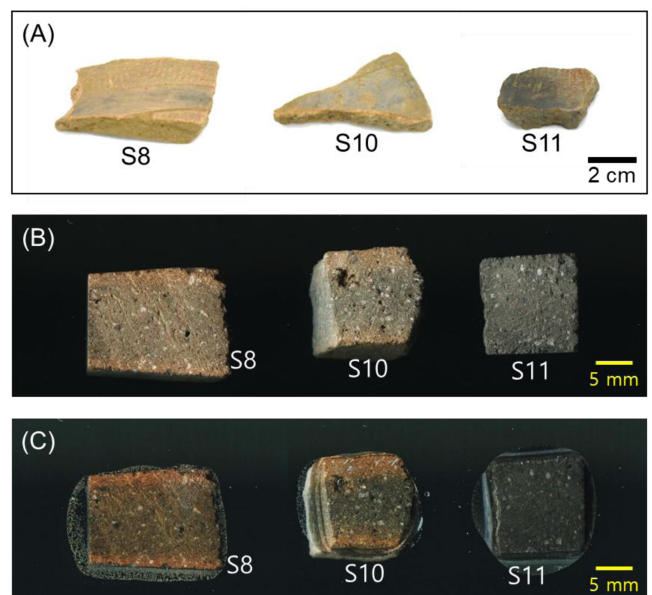
Lorentzian lines.

## 3. Results and Discussion

### 3.1. Cross-sectional observation and elemental distribution

Figure 2a shows the images of the pottery sherds. The color of the outer and inner surfaces of the pottery sherds is generally affected by the use of the vessels, the surface treatment during pottery manufacture and the burial history. Therefore, they cannot provide information about the firing processes of the ceramic, only the color of the cross-section reflects the firing process and the color of the clay used [26]. In this study, thus, the description of the color of the sherds is given with respect to only two cross-sectional parts: the outer rim and the body core as shown in Fig. 2b and 2c.

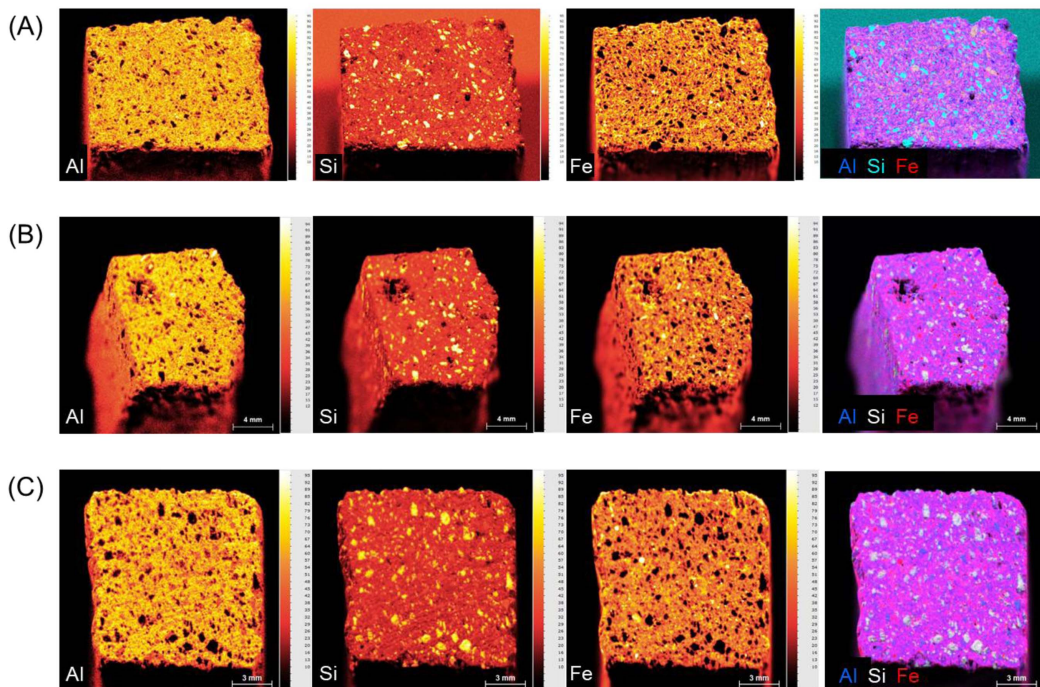
The cross-section of Mombal pottery shows either the alternation of two or three colors with brown, grey, and black hues and a sandwich structure: sherds S8 and S10, or totally uniform color with grey and/or black: sherd S11. In general, the different colored layers in cross-section of the pottery indicate the trace of selective use of colorant raw materials and/or the presence of organic matter [27–32], or the traces of phase transformations of iron oxides within the clay paste that resulted from firing conditions [33–38]. For the latter, red and brown colors are caused by  $\text{Fe}^{3+}$  indicating formation under oxidizing conditions, grey and black colors indicate  $\text{Fe}^{2+}$  and



**Fig. 2.** (Color online) Photographs of the Mombal pottery: (A) pottery sherds, (B) dried cross-section specimens, and (C) wet cross-section specimens.

**Table 2.** Chemical composition of the representative Mombal pottery sherds (wt %).

Sample (cross-sectional part)	SiO <sub>2</sub>	TiO <sub>2</sub>	Al <sub>2</sub> O <sub>3</sub>	Fe <sub>2</sub> O <sub>3</sub> (t)	MnO	MgO	CaO	Na <sub>2</sub> O	K <sub>2</sub> O	P <sub>2</sub> O <sub>5</sub>
S8 (outer)	55.28	2.02	26.38	8.25	0.06	1.26	0.38	-	6.07	0.03
S8 (core)	55.14	2.12	26.29	8.07	0.06	1.46	0.39	-	6.15	0.04
S10 (outer)	58.61	1.32	29.38	5.09	0.04	0.46	0.23	-	4.70	-
S10 (core)	57.18	1.24	30.48	5.35	0.04	0.53	0.26	-	4.75	-
S11 (whole body)	61.05	1.11	32.16	2.93	0.02	-	0.22	-	2.40	-

**Fig. 3.** (Color online) Major element distribution maps of the cross-section of pottery sherds: (A) S8, (B) S10, and (C) S11.

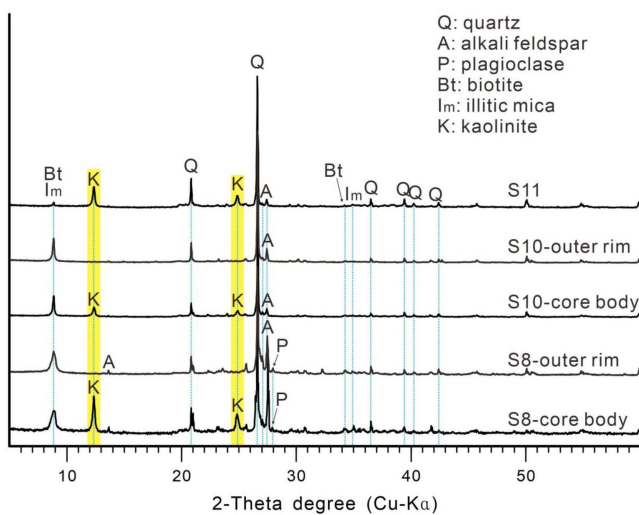
reducing conditions.

Table 2 and Fig. 3 represent the chemical composition and the elemental distribution of each pottery specimens, respectively. The major element composition showed no significant differences between the different colored surface rim and body cores. In particular, the most abundant elements, including Si, Al, and Fe, were evenly distributed across the whole pottery body; excluding quartz particles that showed higher Si concentration. This elemental distribution of pottery sherds showed that silicate minerals, such as quartz, alumino-silicate (principally feldspar) and phyllosilicate (including clay minerals), are the main component. Furthermore, the iron-containing particles are observed in an evenly dispersed pattern with the alumino-silicate particles without forming large-sized aggregates and/or single particles. This indicates that raw clay containing mineral particles with homogeneously

coated iron oxide was used for all samples. Moreover, it is considered that they were prepared in a single clay paste without other chromatic materials added to the surface. In addition, with regard to the non-detection of Na, it may be attributed to the extremely low content of Na-containing minerals and/or the limited resolution of the instrument for detecting trace amounts of light elements.

### 3.2. Mineral composition

The result of bulk powder XRD for each specimen are illustrated in Fig. 4. Overall, the mineral phases of quartz (SiO<sub>2</sub>), feldspar [mainly composed of alkali feldspar (KAlSi<sub>3</sub>O<sub>8</sub>) and some trace of plagioclase (NaAlSi<sub>3</sub>O<sub>8</sub>)], and micaceous minerals [biotite, K(Mg,Fe)<sub>3</sub>(AlSi<sub>3</sub>O<sub>10</sub>)-(F,OH)<sub>2</sub>, in particular] were identified in overall. In our XRD results, particularly the composition of feldspar, are



**Fig. 4.** (Color online) X-ray diffraction patterns of the Mombal pottery sherds.

consistent with the previous research [6], where optical microscopy and XRD of bulk samples showed the presence of microcline and very rare plagioclase has been found in optical microscopy. In addition, the observed mineral composition suggests that the parent rock parent from which the raw clays were derived is an acid granite and/or granitic rock; this suggestion is in accordance with the regional geology [6].

As the most significant difference in the mineral composition within each layer of pottery sherds, it is presented that kaolinite  $[Al_2Si_2O_5(OH)_4]$  was not detected in the reddish/light brown colored outer rim layer of samples S8 and S10. As shown in Table 2, no dramatic difference in  $Al_2O_3$  content was observed between the surface and core regions of each sherd. This finding suggests that the absence of kaolinite may result from its complete thermal decomposition and/or transformation to levels below the detection limit through metakaolinitization. Metakaolinite ( $Al_2Si_2O_7$ ; an amorphous phase not detectable by XRD) is produced by the dehydroxylation of kaolinite at temperatures above 550 °C, and further heating to approximately 900-1,000 °C leads to the development of new phases such as mullite or  $\gamma$ -alumina [39-40]. Therefore, the absence of kaolinite and mullite while the presence of mica in the XRD results indicates firing temperatures above 550 °C and below 900 °C [41-45].

In consequence, this result indicates that the thermal reaction of the ceramic body, may vary from each part, depending on the firing intensity (maximum temperature, duration period, distance from heat source, etc.). Therefore, for a more specific evaluation of ceramic processing,

a separate investigation of distinct minerals for each part (outer part and core of ceramic body) is required to be consider thermal parameters. As examples in present study, if powder samples including whole ceramic body were used, all of the Mombal ceramics in this study would be interpreted as being fired at less than 550 °C due to the detection of kaolinite which decompose between 350 to 500 °C in CaO poor clays and disappears before 500 °C or around 550 °C but never resist above 600 °C [41].

As one exception in the present work, we note that sherd S11 is described as a single layer, because the distinction between surface and body is not clear; the presence of kaolinite suggests that the firing temperature of this sherd is less than 550 °C but at least 400 °C, when the sintering reaction starts, preventing its disintegration [33].

However, unfortunately, the traces of iron-oxide minerals cannot be taken into consideration for the mineralogical classification. The absence of hematite ( $\alpha$ - $Fe_2O_3$ ) and magnetite ( $Fe_3O_4$ ) phases in the XRD results of brown and black colored sherd can be explained by a quantity lower than the detection limit of XRD and their poorly crystallized forms in clayey soil [46-48]. Moreover, these mineral components—as a mineralogical indicator of coloring materials in ceramic body—have yet to be proved with scientific data, despite the previous multi-analytical approaches on the Cameroonian archaeological ceramics [6, 49-51]. The first answer about to this enigma will be given by the results of Mössbauer spectroscopy.

### 3.3. Detection and identification of Fe-compounds phase

As mentioned above, accurately qualifying and quantifying the iron mineral phases in clay can hardly be determined using general standard mineralogical techniques such as X-ray and electron diffractions, chemical extraction, optical and electron microscopy, and magnetic approaches. This is because these methods are frequently below the detection limit of non-silicate iron compounds – including free iron, weakly crystallized iron oxides and hydroxides, superparamagnetic amorphous and/or nano-sized particles, and presence of impurities [52, 53]. Therefore, Mössbauer spectroscopy is an informative method for a more complete picture of the state of iron compounds in clay raw materials of archaeological ceramics [34-38].

Table 3 summarizes the parameters obtained from the Mössbauer spectra (Fig. 5 to 7). The Mössbauer spectra from each pottery sherd consists of several sub-spectra that are overlapped on each other showing that multiple

**Table 3.** RT Mössbauer parameters of the representative Mombal pottery sherds.

Sample	Spectra	IS (mm/s)	QS (mm/s)	H <sub>hf</sub> (kOe)	A (%)	Phase of iron compounds	Fe <sup>3+</sup> /Fe <sup>2+</sup>
S8 (outer)	D1	0.25	0.87	-	45.79	Fe <sup>3+</sup>	22.11
	D2	0.29	1.32	-	30.72	Fe <sup>3+</sup>	
	D3	1.04	2.40	-	3.46	Fe <sup>2+</sup>	
	S1	0.27	-0.10	485.9	20.03	$\alpha$ -Fe <sub>2</sub> O <sub>3</sub>	
S8 (core)	D1	0.24	0.72	-	44.09	Fe <sup>3+</sup>	7.23
	D2	0.30	1.20	-	29.84	Fe <sup>3+</sup>	
	D3	1.01	2.28	-	10.23	Fe <sup>2+</sup>	
	S1	0.27	-0.10	485.8	15.84	$\alpha$ -Fe <sub>2</sub> O <sub>3</sub>	
S10 (outer)	D1	0.27	0.86	-	59.91	Fe <sup>3+</sup>	23.51
	D2	0.22	1.29	-	36.01	Fe <sup>3+</sup>	
	D3	0.96	2.31	-	4.08	Fe <sup>2+</sup>	
	S1	0.29	0.84	-	58.72	Fe <sup>3+</sup>	
S10 (core)	D2	0.29	1.37	-	26.62	Fe <sup>3+</sup>	5.82
	D3	0.96	2.31	-	14.66	Fe <sup>2+</sup>	
	D1	0.10	0.43	-	29.75	Fe <sup>3+</sup>	
	S1	0.26	-0.10	485.1	18.71	$\alpha$ -Fe <sub>2</sub> O <sub>3</sub>	
S11 (whole body)	D2	0.34	0.85	-	32.99	Fe <sup>3+</sup>	3.38
	D3	1.03	2.43	-	18.55	Fe <sup>2+</sup>	
	D1	0.26	-0.10	485.1	18.71	$\alpha$ -Fe <sub>2</sub> O <sub>3</sub>	

iron containing phases are present.

Figure 5 presents the room-temperature (RT) Mössbauer spectra of the (a) reddish brown outer rim and (b) dark brown to grey core body in the sherd S8. The spectra in the sherd S8 reveal three doublets (D1, D2 and D3) arising from quadrupole splitting in paramagnetic states and a single magnetically split sextet (S1). The isomer shift (IS) values for D1 and D2 are 0.24 to 0.25 and 0.29 to 0.30, respectively. The computed parameters indicate that for each component, D1 and D2 correspond to Fe<sup>3+</sup> in superparamagnetic iron oxides/hydroxides and iron within the phyllosilicate structure of fine clay minerals [53-63].

Paramagnetic doublet D3 is associated with Fe<sup>2+</sup>, which usually covers the isomer shift in the range of 0.7 to 1.2 mm/s. In addition, the hyperfine magnetic field (H<sub>hf</sub>) values of the magnetic sextet S1 are 485.8 to 485.9 kOe in the outer rim and body core, respectively, and its (QS) and IS values are -0.10 and 0.27 mm/s, indicating it represents hematite [53]. As presented in Table 2, the quantitative data obtained from the Mössbauer parameters of Sherd S8 show a distinct decrease in Fe<sup>2+</sup> and a corresponding increase in Fe<sup>3+</sup> toward the outer rim relative to the body core. In particular, the Fe<sup>3+</sup>/Fe<sup>2+</sup> ratios were 22.11 in the outer rim and 7.23 in the body core.

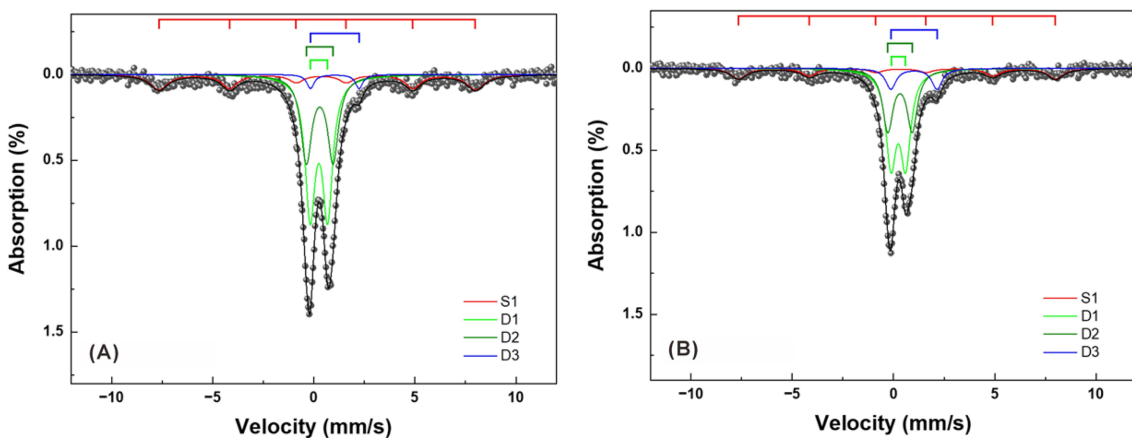


**Fig. 5.** (Color online) Mössbauer spectra of pottery sherd S8 at room temperature: (A) outer rim and (B) body core.

These Mössbauer spectroscopic results clearly indicate that the outer margin underwent a higher degree of oxidation than the core region [37, 64, 65].

As shown in Fig. 6, the decomposed spectra of the sherd S10 show a superparamagnetic behavior, which dominated by three quadrupole doublets; whose parameters are consistent with superparamagnetic  $\text{Fe}^{3+}$  of iron oxides and it in the phyllosilicates of fine clay (D1 and D2), while the  $\text{Fe}^{2+}$  (D3) relates to the release of Fe (II) from aluminosilicate minerals, which caused by redox processes, hydrolysis, and other weathering phenomena of clayey soil [53-63]. The IS and QS values of each doublet component (D1, D2, and D3) are 0.27 to 0.29, 0.22 to 0.29, 0.96, and 0.84 to 0.86, 1.29 to 1.37, 2.31, respectively. According to the quantitative Mössbauer data (Table 2), the  $\text{Fe}^{2+}/\text{Fe}^{3+}$  ratios of Sherd S10 were 23.51 and 5.82 in the outer margin and the core, respectively. This result suggests that, as in the case of sherd S8, the outer margin of sherd S10 exhibits more advanced oxidation compared to its core region. In contrast to that

of the sherd S8, the RT Mössbauer spectra of the sherd S10 did not contain a magnetic sextet assigned to hematite in either the outer rim and the body core. The superparamagnetic behavior observed in the Mössbauer spectrum of Sherd S10 reflects the magnetic characteristics of very small ferromagnetic or ferrimagnetic nanoparticles [53, 64, 66-69]. This indicates that the ceramic sherd was not sufficiently heated to fully magnetize the Fe-oxides and Fe-compounds dispersed within the raw clay, thereby accounting for the absence of spectral components attributable to hematite.

Figure 7 shows the RT Mössbauer spectrum, which represents the composition of iron compounds in the whole clay paste of black colored pottery sherd S11. Its spectra are represented by a superposition of the lines of  $\text{Fe}^{3+}$  and  $\text{Fe}^{2+}$  doublets (D1, D2, and D3; which IS values are 0.10, 0.34, and 1.03 mm/s, respectively). In the Mössbauer spectra of sherd S11, the doublets assigned to  $\text{Fe}^{3+}$  are attributed to iron present within clay minerals and to weakly crystallized superparamagnetic iron oxides ( $\text{Fe}_2\text{O}_3$ ) [53, 64, 66-69]. Meanwhile, the  $\text{Fe}^{2+}$  component is interpreted as arising not from Fe (II)-bearing silicate minerals in the raw clay, but rather from the reduction of free iron derived from such mineral components or superparamagnetic iron oxides [35, 37, 65, 70]. In this regard, Sherd S11—with its uniformly black-colored body—exhibits an  $\text{Fe}^{3+}/\text{Fe}^{2+}$  ratio of 3.38, implying that it experienced the most pronounced reduction among all sherd and regions analyzed in this study. Furthermore, in contrast to Sherd S8 and S10, which display signs of surface oxidation, this result indicates that a reducing atmosphere was maintained during the firing process. In addition to these doublets, a distinct hematite sextet (S1)

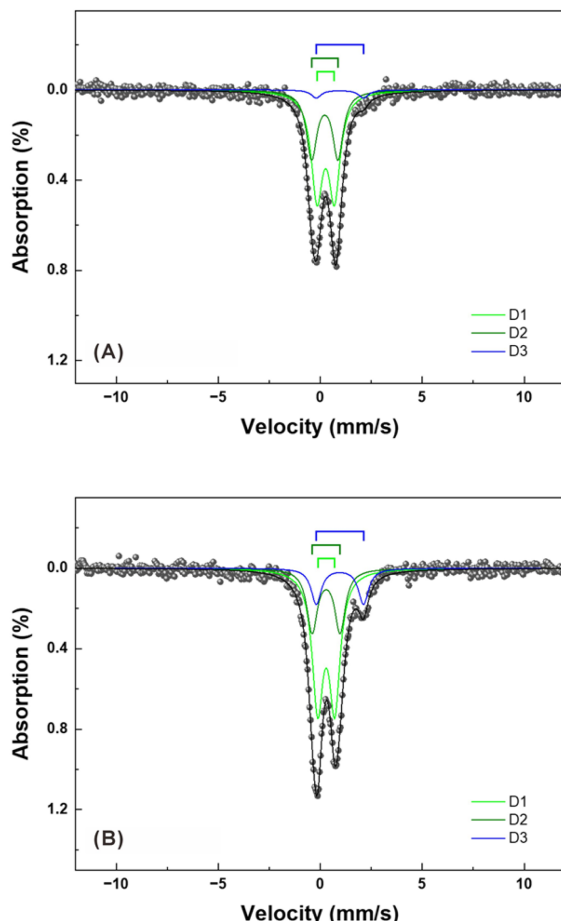


**Fig. 6.** (Color online) Mössbauer spectra of pottery sherd S10 at room temperature: (A) outer rim and (B) body core.

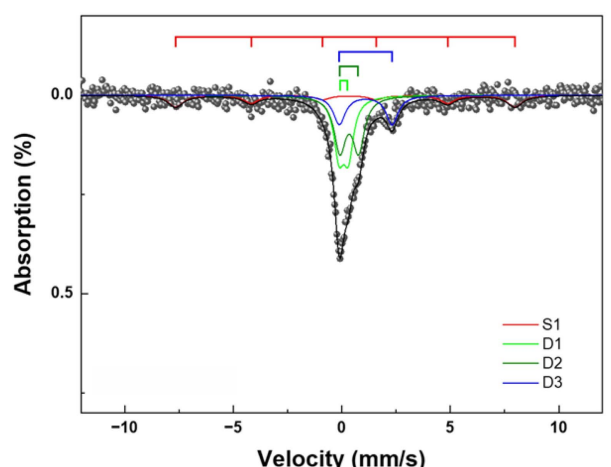


**Fig. 7.** (Color online) Mössbauer spectrum of pottery sherd S11 at room temperature.

was observed, which  $H_{hf}$ , QS, and IS values are 485.1 kOe, -0.10, and 0.26, respectively. As illustrated in Fig. 4, the identification of hematite—undetected in the XRD results—was made possible owing to the high sensitivity of Mössbauer spectroscopy toward iron-bearing phases. Nevertheless, a more detailed assessment of phases exhibiting ferrimagnetic and/or ferromagnetic behavior would require additional magnetic investigations, such as Vibrating Sample Magnetometry (VSM) and low-temperature Mössbauer spectroscopy. Regarding the hematite component assigned to the sextet observed in the reduced pottery sherd S11, further discussion is warranted to evaluate the potential coexistence of magnetite and maghemite ( $\gamma$ -Fe<sub>2</sub>O<sub>3</sub>) formed through reduction processes.

In our study, Mössbauer spectroscopic data demonstrate that iron forms beyond the silicate minerals, as free iron and iron-oxide phases in pottery sherds from the Mombal region. Moreover, quantitative assessments of each iron phase allowed us to calculate their contents, which are used as a characteristic associated with firing parameters [34-38]. The examined data from sherds S8 and S10, characterized by a sandwich structure, show a decreasing trend of Fe<sup>2+</sup> in their reddish-/light-colored outer rim. In contrast, the area of Fe<sup>3+</sup> doublets related to the poorly crystalline iron oxides/hydroxides increase as well as the area of hematite sextet (only in the sherd S8). An increased spectra area of Fe<sup>3+</sup> and hematite in the reddish-/light-brown colored outer rims as compared with the dark colored body cores is the result of iron oxidizing during pottery manufacturing under firing conditions. In addition, according to Mössbauer data, the Fe<sup>2+</sup> content in the black colored pottery sherd S11 amounted to 18.55%; in dark colored body core of sandwich structured sherd, to 10.23-14.66%; and in oxidized outer rim of sherds S8 and S10, to 3.46 and 4.08%, respectively. All this suggests that an increase in the spectral area of Fe<sup>2+</sup> in the dark colored pottery body reflects the response of iron-containing compounds to a change in the redox conditions [48, 71].

#### 3.4. Clay processing for pottery manufacturing in Mombal region

The estimation of the ceramic firing process can be inferred from the mineralogical changes of a clayey material after firing [72-74]. As discussed earlier, the chemical and mineralogical composition of the Mombal pottery in the present study indicated that they were manufactured mainly from local clay without the additional coloring materials to the clay paste.

In addition, the presence/absence of kaolinite and micaceous minerals (the mineralogical indicators) was

considered as an archaeo-thermometer on the Mombal pottery. In particular, we suggested a somewhat different approach to estimating the firing temperature compared to the approach used in the previous study [6]. The key point was a bi-fractional investigation of the outer part and inner part of the cross-sectional specimen, because different firing traces are observed at each part. Therefore, the evaluated firing temperature showed a distinct difference according to the characteristics of each part of the pottery body. The estimated firing temperature of the reddish- and light- brown colored outer rim of sherds S8 and S10 was between 550 to 900 °C. In contrast, the grey to black colored core body of sherds S8, S10, and S11 considered to have been fired below 550 °C. This is the key of ceramic thermal reactions of the Mombal region. It indicates that heating traces of the pottery differ from each part due to irregularities in firing intensity. Therefore, simple open firing system could have been used as heating process [75, 76]. Furthermore, previous works on Mombal and other Cameroonian archaeological ceramics suggested two different types of firing systems in the excavation: bon-firing and pit-firing systems [6, 49, 50]. Moreover, archaeological and ethnographic works also indicated two types of firing systems used during the Neolithic period: bon-firing and pit-firing [8-18].

As noted above, red and brown hues in ceramic bodies result from the presence of Fe<sup>3+</sup> associated with ferric oxides (Fe(III)-oxides), indicating firing under oxidizing conditions. In contrast, grey and black colors arise from Fe<sup>2+</sup> due to the presence of dark-colored iron oxides (Fe(II,III)-oxides and/or Fe(II)-oxides), which reflect formation under reducing conditions [33-38]. In the present study, the Mössbauer spectroscopic data revealed the presence and quantitative values of these coloring factors in the Mombal ceramics, which were not detected by standard mineral analysis techniques previously conducted on them.

Pottery sherds S8 and S10 correspond mostly to cross sections with a grey or black core body and colored margins; reddish and light brown, respectively. This sandwich structure of the pottery fracture section is related to a short duration of firing and lower firing temperature or insufficient oxidation [33]. Consequently, the color of the cross sections—brownish, blackish, and brownish at the inner rim, body core, and outer rim, respectively—is explained by heating without and cooling with oxygen available; the oxygen reacts with both margins during cooling. These variation in the color of the ceramic body may be related to a bon-firing system where the control of oxygen and firing time are difficult to manage [73]. Furthermore, the redder coloration

observed on the fracture surface of Sherd S8 compared to that of Sherd S10 is interpreted as reflecting a higher proportion of  $\text{Fe}^{3+}$  and  $\alpha\text{-Fe}_2\text{O}_3$  phases (Table 3, Figs. 6 and 7), which likely resulted from oxidation reactions occurring under longer firing durations and elevated firing temperatures [37, 64, 65].

In contrast, the pottery sherd S11 has a black to dark grey color of the cross-sectional surface, indicating a reducing firing condition. In the pit-firing system, the simplest and most efficient way to maintain a reducing atmosphere during heating and cooling is to cover the pit on top in order to create a confined system [77]. In this regard, our results confirm that the past potters who manufactured Mombal pottery made intentional technical choices regarding firing systems. However, the fundamental reasons behind their choices, such as bon-firing and pit-firing, remain unclear.

#### 4. Conclusion

In this study, we used scientific tools to examine characteristic pottery fragments from the Boutila site in the Mombal region of eastern Cameroon. Sample characterization was performed using cross-sectional observation, XRF element mapping, XRD, and Mössbauer spectroscopy. By comparing our results with the archaeological record, we reconstructed the production process of pottery from the Mombal. Our findings indicate that Mombal pottery were mainly manufactured from local clay without the additional coloring materials to the clay paste. In addition, firing condition of the pottery showed significant differences between the outer and inner part of the sherds. Based on the absence/presence of kaolinite as a mineralogical thermo-indicator, the estimated firing temperature of the brown colored outer rim of sandwich-structured pottery sherds was between 550 and 900 °C. In contrast, its grey to black-colored core body is considered to be fired below 550 °C but above at least 400°C. In the case of black-colored monochrome pottery, the constructive firing temperature was below 550 °C, with a lower limit of 400°C. Furthermore, the qualitative and quantitative compositions of the iron compounds confirm that the redox conditions were also not homogeneous during their firing process of Mombal pottery. According to each partial color of the pottery body, reddish- and light-brown colored outer part suggested oxidizing condition with increase of  $\text{Fe}^{3+}$  and hematite, whereas dark-colored inner core part indicated a reducing firing condition based on relatively higher content of  $\text{Fe}^{2+}$ .

These variations in the firing intensity and the color of each pottery body confirmed the use of an open-firing

system on the ground, where the control of oxygen and firing time are difficult to manage. In consequence, their differences in the mineralogical characteristics, particularly in the color scheme between sandwich- and monochrome- structure, demonstrated the possibility of intentional choices of firing techniques of the past Mombal potters, such as bon-firing and pit-firing.

#### Acknowledgements

This work was supported by the Basic Research Project “Research on the development and dissemination of contents responding to public demand and social issues in geoscience (Project No. GP2025-001)” of the Korea Institute of Geoscience and Mineral Resources (KIGAM).

#### References

- [1] O. Langlois and C. Mbida Mindzié, *Archéologie, Les Éditions J. A.*, Paris (2006) pp. 68-69.
- [2] G. Loumpet, Dissertation, *Eléments de synthèse pour un cadre paléoclimatique et paléoécologique quaternaire au Cameroun. Première approche d'une industrie lithique ancienne dans les dépôts alluviaux de Biti en haute-sangha (Est-Cameroun-Ouest RCA)*, Université de Paris I, Panthéon-Sorbonne, France (1987).
- [3] R. Assombang, M. Delneuf, and C. Mbida-Mindzie, rapport final (2002).
- [4] A. Mezop, Dissertation, *Etude préliminaire des poteries anciennes de Wele Maroua (Est-Cameroun)*, Université de Yaoundé I, Cameroon (2002).
- [5] C. Lako, Dissertation, *Reconnaissance archéologique dans l'Est Cameroun. Etude des sites de Mombal*, Université de Yaoundé I, Cameroon (2005).
- [6] Z. L. Epossi Ntah, Dissertation, *Archaeometrical studies: petrography, mineralogy and chemistry of selected ceramic sherds and clay samples from Cameroon - Regions of Mombal, Mfomakap and Zamala-*, University of Leipzig, Germany (2012).
- [7] Z. L. Epossi Ntah, R. Sobott, B. Fabbri, and M. Elouga, *Annales* **20**, 1 (2018).
- [8] O. P. Gosselain, Dissertation, *Identités techniques, le travail de la poterie au Cameroun meridional*, Université Libre de Bruxelles, Belgium (1995).
- [9] D. Nicholas, K. Gavua, A. Scott MacEachern, and J. Sterner, *Can. J. Archaeol.* **15**, 171 (1991).
- [10] O. P. Gosselain, *Man* **27**, 559 (1992).
- [11] O. P. Gosselain, *J. Archaeol. Method. Theory.* **7**, 187 (2000).
- [12] J. W. Arthur, *J. Anthropol. Archaeol.* **35**, 106 (2014).
- [13] A. Delvoye, A. Mayor, and N. S. Guèye, *J. Anthropol. Archaeol.* **75**, 101602 (2024).
- [14] B. Nxumalo, *Afr. Archaeol. Rev.* **40**, 89 (2023).

[15] R. T. Nyamushosho, Aspects of consumption and symbolism: a ceramic ethnoarchaeological study of ritual vessels among the Saunyama of north-eastern Zimbabwe, *Langaa RPCIG*, Bamenda (2017) pp. 241-276.

[16] R. T. Nyamushosho and S. Chirikure, *Quat. Int.* **555**, 150 (2020).

[17] E. M. Perez-Monserrat, V. Baratella, L. Maritan, and M. Vidale, *App. Clay. Sci.* **255**, 107418 (2024).

[18] I. Pikirayi and A. Lindahl, *Afr. Archaeol. Rev.* **30**, 455 (2013).

[19] D. A. Santacreu, Materiality, Techniques and Society in the pottery production: The Technological Study of Archaeological Ceramics through Paste Analysis, De Gruyter Open Ltd., Warsaw/Berlin (2014) p. 336.

[20] A. Livingstone-Smith, *Archaeometry* **42**, 21 (2000).

[21] B. Pfaffenberger, *Annu. Rev. Anthropol.* **21**, 491 (1992).

[22] P. M. Rice, Some reflections on change in pottery producing systems, Institute for Pre- and Proto-history, Amsterdam (1984) pp. 231-293.

[23] M. A. Dobres, Technology and social agency, Blackwell Publishers, New Jersey (2000) p. 315.

[24] O. P. Gosselain, *Poteries du Cameroun méridional. Styles techniques et rapports à l'identité*, C N R S, Paris (2002) p. 254.

[25] P. Burhman, P. E. Copet-Rougier, and P. Noss, *Paideuma* **32**, 87 (1986).

[26] R. Martineau and P. Petrequin, La cuisson des poteries néolithiques de Chalain (Jura), approche expérimentale et analyse archéologique, APDCA, Nice (2000) pp. 337-358.

[27] F. M. Hawley, *Am. Anthropol.* **31**, 731 (1929).

[28] J. D. Stewart and K. R. Adams, *Am. Antiq.* **64**, 675 (1999).

[29] M. Pendleton, D. K. Washburn, E. A. Ellis, and B. B. Pendleton, *Microsc. Today* **20**, 32 (2012).

[30] M. Pendleton, D. K. Washburn, E. A. Ellis, and B. B. Pendleton, *Yale J. Biol. Med.* **87**, 15 (2014).

[31] L. Rosado, J. V. Pevenage, P. Vandenabeele, A. Candeias, M. D. C. Lopes, and D. Tavares, *Measurement* **118**, 262 (2017).

[32] M. Spataro, M. Cubas, O. E. Craig, J. C. Chapman, A. Boroneant, and C. Bonsall, *Archaeol. Anthropol. Sci.* **11**, 6287 (2019).

[33] G. Artioli, *Scientific methods and cultural heritage- An introduction to the application of materials science to the archaeometry and conservation science*, Oxford University Press, Oxford (2010) p. 536.

[34] N. H. J. Gangas, A. Kostikas, A. Simopoulos, and J. Vocotopoulou, *Nature* **229**, 485 (1971).

[35] A. Kostikas, A. Simopoulos, and N. H. J. Gangas, *J. Phys.* **35**, 107 (1974).

[36] R. Venkatachalam, D. Gournis, C. Manoharan, S. Dhanapandian, and K. Deenadayalan, *Indian J. Phys.* **78**, 1371 (2004).

[37] D. H. Moon, M. S. Lee, and H. G. Cho, *J. Radioanal. Nucl. Chem.* **330**, 419 (2021).

[38] H. Choi, G. M. Sun, and Y. R. Uhm, *J. Radioanal. Nucl. Chem.* **332**, 5119 (2023).

[39] A. K. Chakravorty and D. K. Ghosh, *J. Am. Ceram. Soc.* **71**, 978 (1988).

[40] S. Lee, Y. J. Kim, and H. S. Moon, *J. Am. Ceram. Soc.* **82**, 2841 (1999).

[41] E. Murad and U. Wagner, *Hyperfine Interaction* **45**, 161 (1989).

[42] M. Maggetti, H. Westley, and J. S. Olin, *Provenance and technical studies of Mexican majolica using elemental and phase analysis*, American Chemical Society, Washington (1984) pp. 151-191.

[43] U. Hertli, M. Maggetti, A. Jornet, and G. Galetti, *Proceedings of 4th European Meeting on Ancient Ceramics: Archaeological and archaeometrical studies*, Andorra (1997) pp. 168-174.

[44] Y. Maniatis, A. Simopoulos, A. Kostikas, and V. Perdikatsis, *J. Amer. Ceram. Soc.* **66**, 773 (1983).

[45] M. Bellotto, A. Gualtieri, G. Artioli, and S. M. Clark, *Phys. Chem. Miner.* **22**, 207 (1995).

[46] T. Alekseeva, A. Alekseev, B. Maher, and V. Demkin, *Palaeogeogr. Palaeoclimatol. Palaeoecol.* **249**, 103 (2007).

[47] Z. Jiang, Q. Liu, A. P. Roberts, M. J. Dekkers, V. Barrón, J. Torrent, and S. Li, *Rev. Geophys.* **60**, e2020RG000698 (2021).

[48] V. V. Malyshev and A. O. Alekseev, *Eurasian Soil Sci.* **57**, 1461 (2024).

[49] Z. L. Epossi Ntah, G. Cultrone, and E. Ndome Effoudou-Priso, *Archaeometry online*, 1 (2025).

[50] Z. L. Epossi Ntah and G. Cultrone, *Herit. Sci.* **12**, 6 (2024).

[51] Z. L. Epossi Ntah, R. Sobott, B. Fabbri, and K. Bente, *Cerâmica* **63**, 413 (2017).

[52] Y. N. Vodyanitskii and S. A. Shoba, *Eurasian Soil Sci.* **47**, 573 (2014).

[53] M. Mashlan, R. Zboril, L. Machala, M. Vujtek, J. Walla, and K. Nomura, *J. Metastab. Nanocryst. Mater.* **20**, 641 (2004).

[54] A. A. Novakova, V. O. Denisov, N. M. Boeva, and A. Tsatskin, *Crystallogr. Rep.* **65**, 376 (2020).

[55] E. Murad, *Properties and behavior of iron oxides as determined by Mössbauer spectroscopy*, Springer, Dordrecht (1988) pp. 309-350.

[56] X. Cao, R. Prozorov, Y. Koltypin, G. Kataby, I. Felner, and A. Gedanken, *J. Mater. Res.* **12**, 402 (1997).

[57] P. Ayyu, M. Multani, M. Barma, V. R. Palkar, and R. Vijayaraghavan, *J. Phys. C Solid State Phys.* **21**, 2229 (1988).

[58] M. F. Hansen, C. B. Koch, and S. Mørup, *Phys. Rev. B Condens. Matter* **62**, 1124 (2000).

[59] F. Bødker, M. F. Hansen, C. B. Koch, K. Lefmann, and S. Mørup, *Phys. Rev. B Condens. Matter* **61**, 6826 (2000).

[60] L. T. Kuhn, K. Lefmann, C. R. H. Bahl, S. N. Ancona, P. A. Lindgård, C. Frandsen, D. E. Madsen, and S. Mørup,

Phys. Rev. B Condens. Matter **74**, 184406 (2006).

[61] E. Murad and J. D. Fabris, J. Phys. Conf. Ser. **217**, 012066 (2010).

[62] L. Heller-Kallai and I. Rozenson, Phys. Chem. Miner. **7**, 223 (1981).

[63] V. A. Drits, L. G. Dainyak, F. Muller, G. Besson, and A. Manceau, Clay Miner. **32**, 153 (1997).

[64] D. H. Moon, N. R. Lee, W. R. Han, S. J. Kim, and Y. R. Uhm, J. Radioanal. Nucl. Chem. **332**, 5175 (2023).

[65] C. Manoharan, R. Venkatachalapathy, S. Dhanapandian, K. Deena-dayalan, Indian J. Pure. Appl. Phys. **45**, 860 (2007).

[66] E. Murad, Hyperfine Interact. **47**, 33 (1989b).

[67] X. Cao, R. Prozorov, Y. Koltypin, G. Kataby, I. Felner, and A. Gedanken, J. Mater. Res. **12**, 402 (1997).

[68] P. Ayyub, M. Multani, M. Barma, V. R. Palkar, and R. Vijayaraghavan, J. Phys. C Solid State Phys. **21**, 2229 (1988).

[69] M. F. Hansen, C. B. Koch, and S. Mørup, Phys. Rev. B Condens. Matter **62**, 1124 (2000).

[70] S. Nagy, E. Kuzman, T. Weiszburg, M. Gyökeres-Tóth, and M. Riedel, J. Radioanal. Nucl. Chem. **246**, 91 (2000).

[71] V. F. Babanin, V. I. Trukhin, L. O. Karpachevskii, A. V. Ivanov, and V. V. Morozov, Soil Magnetism, Izd. Yarosl. Gos. Tekhn. Univ., Yaroslavl–Moscow (1995) p. 222.

[72] L. Nodari, E. Marcuz, L. Maritan, C. Mazzoli, and U. Russo, J. Eur. Ceram. Soc. **27**, 4665 (2007).

[73] M. Maggetti, C. Neururer, and D. Ramseyer, App. Clay Sci. **53**, 500 (2011).

[74] E. M. Perez-Monserrat, L. L. Crespo-, G. Cultrone, M. A. Paolo, and L. Maritan, J. Archaeol. Sci. Rep. **54**, 104400 (2024).

[75] O. P. Gosselain, J. Archaeol. Sci. **19**, 243 (1992).

[76] J. Mercader, M. Garcia-Heras, and I. Gonzalez-Alvarez, J. Archaeol. Sci. **27**, 163 (2000).

[77] J. Bonzon, Archaeometrical study (petrography, mineralogy and chemistry) of Neolithic Ceramics from Arbon Bleiche 3 (Canton of Thurgau, Switzerland), Université de Fribourg, Fribourg (2005) p. 187.